

Review

# All-Purpose Nano- and Microcontainers: A Review of the New Engineering Possibilities

George Kordas 

Self-Healing Structural Materials Laboratory, World-Class Scientific Center of the Federal State Autonomous Educational Institution of Higher Education, Peter the Great St. Petersburg Polytechnic University, 195251 St. Petersburg, Russia; gckordas@gmail.com

**Abstract:** Recently, a subcategory of nanotechnology—nano-, and microcontainers—has developed rapidly, with unexpected results. By nano- and microcontainers, we mean hollow spherical structures whose shells can be organic or inorganic. These containers can be filled with substances released when given an excitation, and fulfill their missions of corrosion healing, cancer therapy, cement healing, antifouling, etc. This review summarizes the scattered innovative technology that has beneficial effects on improving people's lives.

**Keywords:** nanocontainers; microcontainers; self-healing; cancer; antibacterial; PCM; antifouling; corrosion

## 1. Introduction

The encapsulation of substances in a protective shell has recently become necessary because of the enormous technological possibilities in medicine [1], materials [2], energy [3], antifouling [4], antimicrobials [5], implants [6], the environment [7], etc. As a result, significant progress has also been made in manufacturing containers [8]. The primary method of their four-step production is firstly, the creation of the core; secondly, the coating of the core with the active shell; thirdly, the removal of the core; and finally, encapsulation with the active material. Reference is made here to production because containers can be produced differently, which is not mentioned in this article, e.g., LDH [9,10]. The present review covers the latest development in this technology via four-step production and gives examples of its industrial application. In this paper, we talk about organic and inorganic nanospheres in which each species is better suited to specific applications. CeMo (MBT or 8-HQ) nanospheres are inhibitors for applications in corrosion because they act simultaneously as a cathodic and anodic corrosion inhibitor. This property cannot be derived from the organic nanospheres that are best suited for cancer-fighting applications where we need artificially intelligent nanocontainers to diagnose and fight cancer. Intelligence cannot be obtained by inorganic nanospheres that are better suited to nontherapeutic applications, except for FeO nanospheres, to which hyperthermia can be applied to improve cancer treatment. Here, we can use the EPR effect to enter cancer via hyperthermia to cause destruction. The choice is made according to the problem we want to solve and the expected results. In addition, there are more applications of the nanocontainers not included in this publication, such as storage of hydrogen, food storage, cosmetic storage, etc., which will be the subject of another extensive review.

## 2. Materials and Methods

### 2.1. Inorganic Containers

In producing inorganic nanocontainers, we first produced a polystyrene core with well-known conditions in the bibliography. The polystyrene core's size determines the nanocontainers' final size. An earlier publication investigated the parameters affecting the polystyrene core's size [11]. Terminating the polystyrene core at a negative charge is



**Citation:** Kordas, G. All-Purpose Nano- and Microcontainers: A Review of the New Engineering Possibilities. *Eng* **2022**, *3*, 554–572. <https://doi.org/10.3390/eng3040039>

Academic Editor: Antonio Gil Bravo

Received: 28 October 2022

Accepted: 25 November 2022

Published: 30 November 2022

**Publisher's Note:** MDPI stays neutral with regard to jurisdictional claims in published maps and institutional affiliations.



**Copyright:** © 2022 by the author. Licensee MDPI, Basel, Switzerland. This article is an open access article distributed under the terms and conditions of the Creative Commons Attribution (CC BY) license (<https://creativecommons.org/licenses/by/4.0/>).

essential to deposit the metal oxides' salts on it [8]. Then, the sol-gel method deposited the metal oxide coatings, e.g.,  $\text{Ce}(\text{acac})_3$ . The third stage involved the removal of polystyrene through combustion at  $600^\circ\text{C}$ . Finally, we obtained a shell consisting of  $\text{CeO}_2$  [8],  $\text{CeMo}$  [12],  $\text{TiO}_2$  [13,14],  $\text{CeOTiO}_2$  [11],  $\text{Fe}_2\text{O}_3$  [7],  $\text{SiO}_2\text{CaO}$  [15],  $\text{SiO}_2\text{Na}_2\text{O}$  [6] and  $\text{SiO}_2\text{P}_2\text{O}_5\text{Na}_2\text{O}$  [6], depending on the alkoxides we used. In the final phase, the nanocontainers entered a vacuum chamber, where we received the maximum vacuum value. Then, we broke it with the materials dissolved in alcohols entering the chamber from a funnel, corrosion inhibitors, filling up the nanocontainers with the desired substance. In one case, paraffin entered the  $\text{SiO}_2$  to create phase-change materials [3]. There are cases where the core of  $\text{SiO}_2$  [16] nanocontainers consists of super absorbent polymers (SAP) suited for cement "self-healing" [17,18].

## 2.2. Organic Containers

One uses organic nanocontainers to treat cancer and other diseases [19,20]. The core is composed of PMMA, on which three walls are constructed: one is sensitive to temperature, the second is sensitive to pH, and the third is sensitive to redox. The polymeric nanocontainers are loaded with commercial drugs, such as doxorubicin. The containers are grafted with targeting groups to get bonded to cancer. Furthermore, the nanocontainers are grafted with gadolinium for MRI probes, iron oxide for hyperthermia, Fitch for locating them by fluorescent spectroscopy, etc. The literature has named this system quadrupole stimuli-responsive targeted nanocontainer or Nano4XX (XX = Dox, Daun, Cis, etc.) platforms. The synthesis of such platforms was the subject of several publications in recent literature [1,19]. Figure 1 shows the Nano4XX (XX = Dox, Daun, Cis, etc.) platform and the molecules one uses to produce them [21].

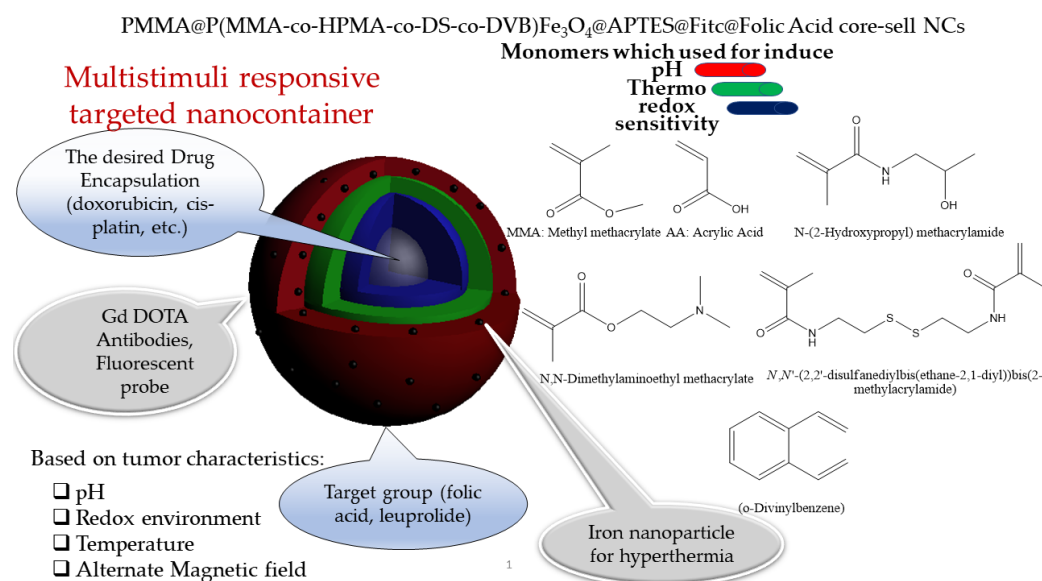


**Figure 1.** Quadrupole stimuli-responsive targeted nanocontainers loaded with cancer therapeutic drugs to treat cancer: the Nano4XX (Dox, Cis, etc.) platform.

## 3. Discussion

### 3.1. Corrosion

Protection against the corrosion of metals is performed by chemical methods designed to replace chromium salts. Several ways have evolved into different metals that offer entirely satisfactory protection. These coatings are, however, passive. They become active when introduced into these nanocontainers filled with inhibitors. With the stimulation caused by corrosion, the inhibitors are released, and thus interrupt the corrosion. This phenomenon is called "self-healing" [22] and is observed in all metals and nanocontainers. [11,13,23–28] Cerium molybdate hollow nanocontainers filled with

2-mercaptobenzothiazole incorporated into epoxy coating deposited onto galvanized steel samples show outstanding inhibition potential after a prolonged corrosion activity. The anodic and cathodic currents determined by SVET showed values close to the noise levels after 20 h of the exhibition to the salt solution until the end of the experiment in 50 h [22]. We attributed the corrosion activity to the organic inhibitor and inorganic inhibitor release of cerium ions from the nanocontainers. Figure 2 shows the SVET measurements of the sample to demonstrate the case.

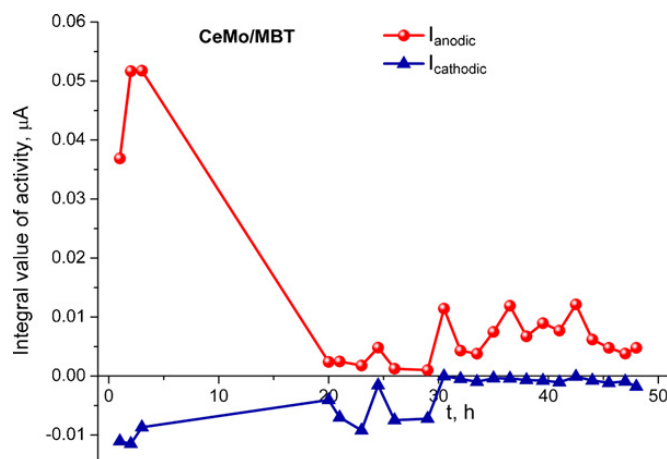


**Figure 2.** Evolution of the total anodic and cathodic current of the sample containing CeMo (MBT).

Today, the technology of nanocontainers is evolving “intelligence” onto them, containing valves sensitive to the pH change of the environment. With this innovation, we hope for a better and more controlled performance of nanocontainers in stimuli due to corrosion. In a recent paper, mesoporous silica nanocontainers were prepared and filled with benzotriazole (BTA) corrosion inhibitors. Nanocontainers contain nanovalves consisting of cucurbit [6] uril (CB [6]) rings attached to the surface of the nanocontainers. They do not undergo a corrosion inhibitor release when the pH is neutral. However, the release rate increases with increasing pH values in an alkaline solution. These nanocontainers respond to the pH, but how much better do they work compared to simple nanocontainers? Especially in commercial paints need to be studied better, but such a study is very innovative. Figure 3 shows their function.

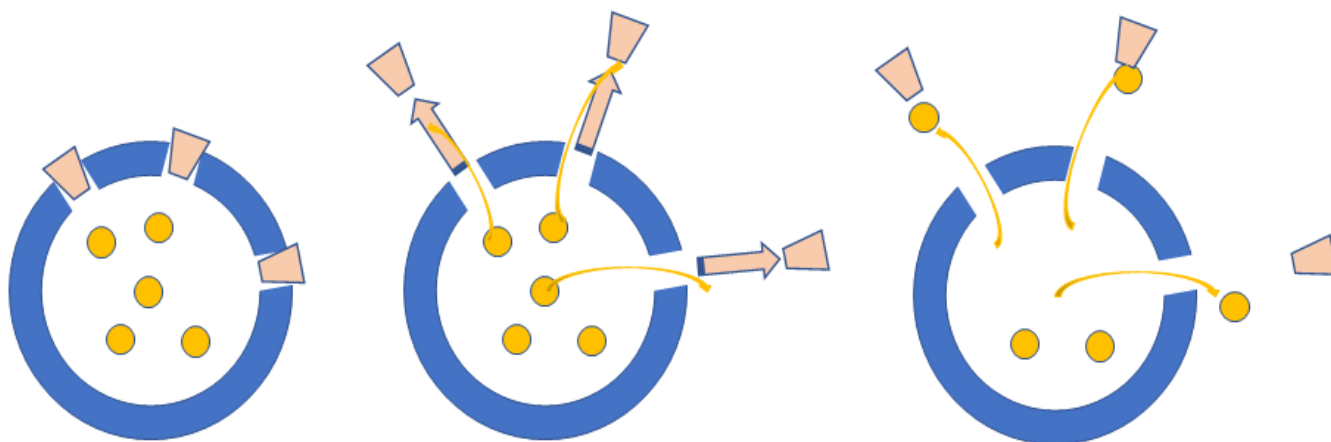


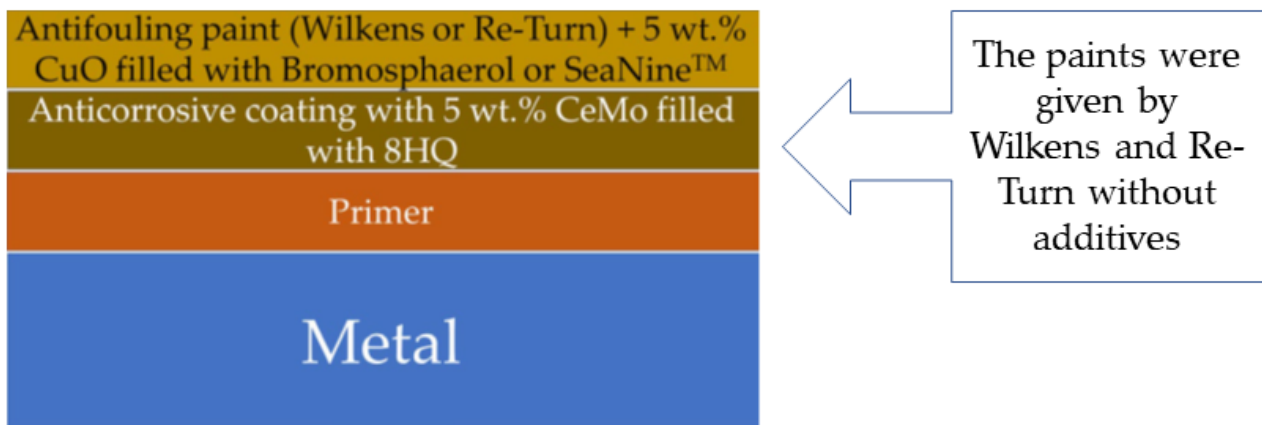
**Figure 3.** Nanovalves sensitive to pH incorporated onto the surface of silica nanocontainers.

A recent review explains in great detail the state of the art of this technology [2]. We refer the reader to an update from this publication if they want to be informed more about the recent development.

### 3.2. Antifouling

When a metal surface encounters the marine environment, it is then quickly covered by a biofilm of microorganisms and further evolves from invertebrate animals that eventually corrode [29]. The result is that ships develop turbulences on their surface, increasing cruising friction, resulting in decreased vessel efficiency, which at the exact same time increases fuel requirements, and ultimately, increases air pollutants. One realizes that this has enormous economic consequences [30]. To avoid this problem, one can use antifouling coatings containing biocides and copper oxide. In this way, one stops the adhesion of organisms to the surfaces for some time. Most biocides effectively target the microorganisms created in the beginning: bacteria, algae, and barnacles. Biocides can be developed by looking for natural compounds that act as antifouling agents [31–39]. The sea has organisms that defend against biological pollution [40,41]. There are a large number of metabolites at sea that have the potential to grow as antifouling agents.

One such compound is bromosphaerol, isolated in algae cultivated in the marine area of Palaiokastritsas in Corfu. These algae were grown in greenhouse conditions to give large quantities, of which bromosphaerol was chemically isolated. Bromosphaerol was encapsulated in copper oxide and zinc oxide nanocontainers to examine the biological aspects of behavior within commercial antifouling paints [4,29]. For this purpose, we used the antifouling bases of the paints of the Wilkens and Re-Turn companies, where we incorporated a small number of CuO and ZnO nanocontainers filled with bromosphaerol. We also used the bases of the two companies and the anticorrosion paints without impurities. We added a small amount of CeMo (8-HQ) to the anticorrosion paint. Figure 4 shows the paint configuration we obtained using basic commercial paints.



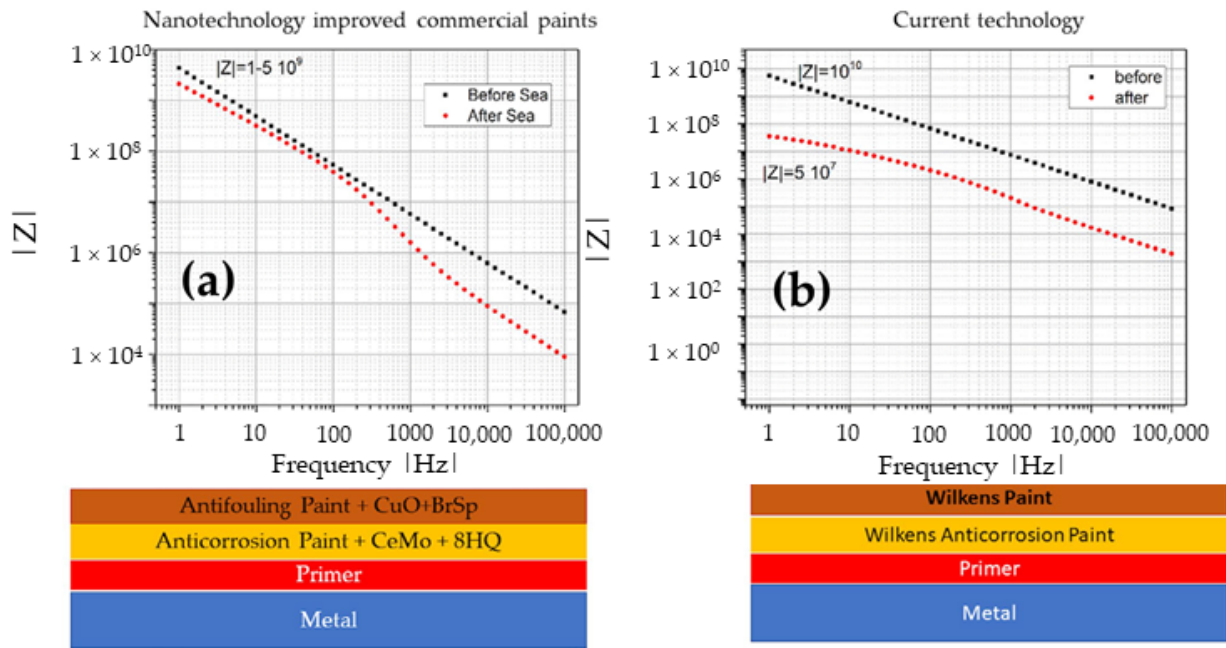
**Figure 4.** Paint configuration for lab testing and used for real-ship paint testing.

Figure 5a,b show the FRA of the two paints, one (a) consisting of the primer, anticorrosion with CeMo (8HQ) layer, and antifouling paint with CuO (Bromosphaerol); and the other (b) the Wilkens commercial paint. Both samples were exposed to the sea for three months. The FRA curves for the samples were the same before exposure to the seawater. On the contrary, the commercial paint's FRA dropped drastically, while our nanocontainer paint's FRA performed much better.

Figure 6 shows the FRA of another two paints, one (a) doped with CuO (S.N.) + ZnO (S.N.) and the other (b) with CuO (S.N.).  $R_p$  is about  $10^{10} \Omega$  before exposure of the samples to seawater. However,  $R_p$  improves for the samples immersed for three months in seawater. This behavior is known as the "self-healing" phenomenon.

The technology is useful when confirmed in practice. However, it was not easy to convince a paint-trading company to paint commercial ships before, firstly because it is dangerous for new technology not to meet the five-year guarantee given by commercial paints, and secondly, because the financial risk is significant if the new technology does not succeed. However, this was made possible by two companies, one Wilkens and the

other Re-Turn, which intervened, and they painted a section of two ships, one traveling to the Adriatic sea and the other to different oceans, with speeds of 14 knots, for one year. Figure 7 shows the sections of the ships painted. It was a pleasant surprise in both cases to see the same results for the parts we painted with the technology of nanocontainers filled with bromophenol. The ships traveled in different marine conditions for a year, and the paints from our laboratory performed better than the commercial paints of the two companies [4,29,42].



**Figure 5.** FRA of paints ((a) nanocontainer technology and (b) commercial paint) before and after immersing the samples in seawater for three points.

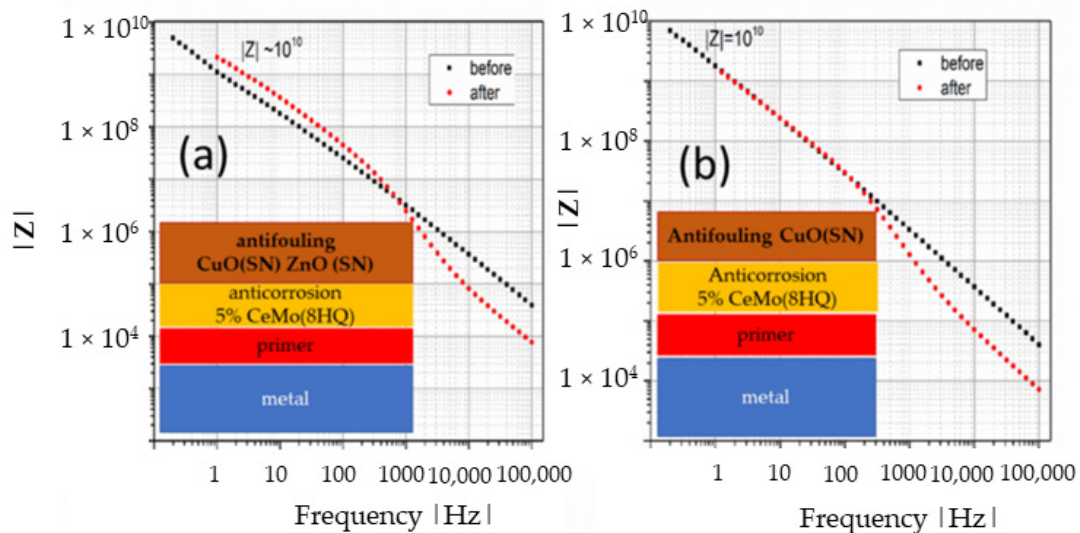


**Figure 6.** FRA of the paints: (a) top layer consisting of CuO (S.N.) and the ZnO (S.N.) nanocontainers, and (b) top layer consisting of CuO (S.N.) nanocontainers.

In a recent paper, Al<sub>2</sub>O<sub>3</sub> and CuO nanoparticles were incorporated as a pigment using linseed alkyd resin as a binder. The samples were immersed in seawater for 120 days, and the properties were studied with modern spectroscopic techniques where a semantic improvement was observed in the antifouling of steel plates using Al<sub>2</sub>O<sub>3</sub> and CuO compared to bare paint. The contact angle increased dramatically, suggesting that the paint

becomes more hydrophobic [43]. These new results confirm the impact of nanocontainers on Wilkens and Re-Turn commercial paints [2,4,24,26,29].



**Figure 7.** The segments of the two ships painted by our nanotechnology.

A relatively recent publication produced a fluorine-free superhydrophobic coating based on the TiO<sub>2</sub> rosin-inoculated nanoparticles. The results were excellent regarding water repellency, which was attributed to the synergistic amplification between natural adhesives and hydrophobic TiO<sub>2</sub> nanoparticles. In addition, the results have shown that such coatings will have great potential to cope with some of the antifouling paints [44].

### 3.3. Antibacterial

Organic and inorganic spheres are the subject of intense scientific activity due to their applications in biology, medicine, photocatalysis, etc. Heterogeneous polymerization methods prepare organic spheres [45–47]. Empty containers are interesting for coatings due to their lower density and optical properties. These can be coated with inorganic shells to modify their properties [48–53]. Photocatalysis uses empty titanium spheres to reduce Cr(VI) to Cr(III), working as an electron acceptor that finally precipitates as solid waste [53]. It is known that TiO<sub>2</sub> appears in nature as brucite (orthorhombic), anatase (quadratic), and rutile (quadratic). Of these three phases, anatase is the most active in photocatalysis. Illumination of TiO<sub>2</sub> by light with an energy higher than 3.2 eV and 3.0 eV for anatase and rutile induces electrons to jump from the valence zone to the conductivity zone, respectively. This transition causes pairs of electrons (e<sup>−</sup>) and electrical holes (h<sup>+</sup>) via photocatalysis. When an organic compound falls on the surface of the photocatalyst, it will react with the produced O<sub>2</sub><sup>−</sup> and OH, transforming into carbon dioxide and water. Thus, the photocatalyst decomposes organic matter in the air, including odor molecules, bacteria, and viruses. The *Escherichia coli* (*E. coli*) bacterium has been used many times for experimental purposes [54].

Hollow-nanosphere titania were used in one study, and their antibacterial activity was evaluated in *E. coli* [55]. Figure 8 shows the survival curve of *E. coli* cells for various conditions. First, the *E. coli* cell concentration was measured in the presence of TiO<sub>2</sub>. One observed about a 20% reduction in *E. coli* cells after 79 min of incubation. Furthermore,

*E. coli* cells were exposed to illumination for 70 min and reduced close to 20%. The *E. coli* cell concentration went down to 0% quickly in the cases illuminated in  $\text{TiO}_2$ . When the light went out after 30 min, followed by an additional 40 min incubation in the dark, one received the same number of viable cells at 70 min as the sample exposed to light for 70 min continuously.

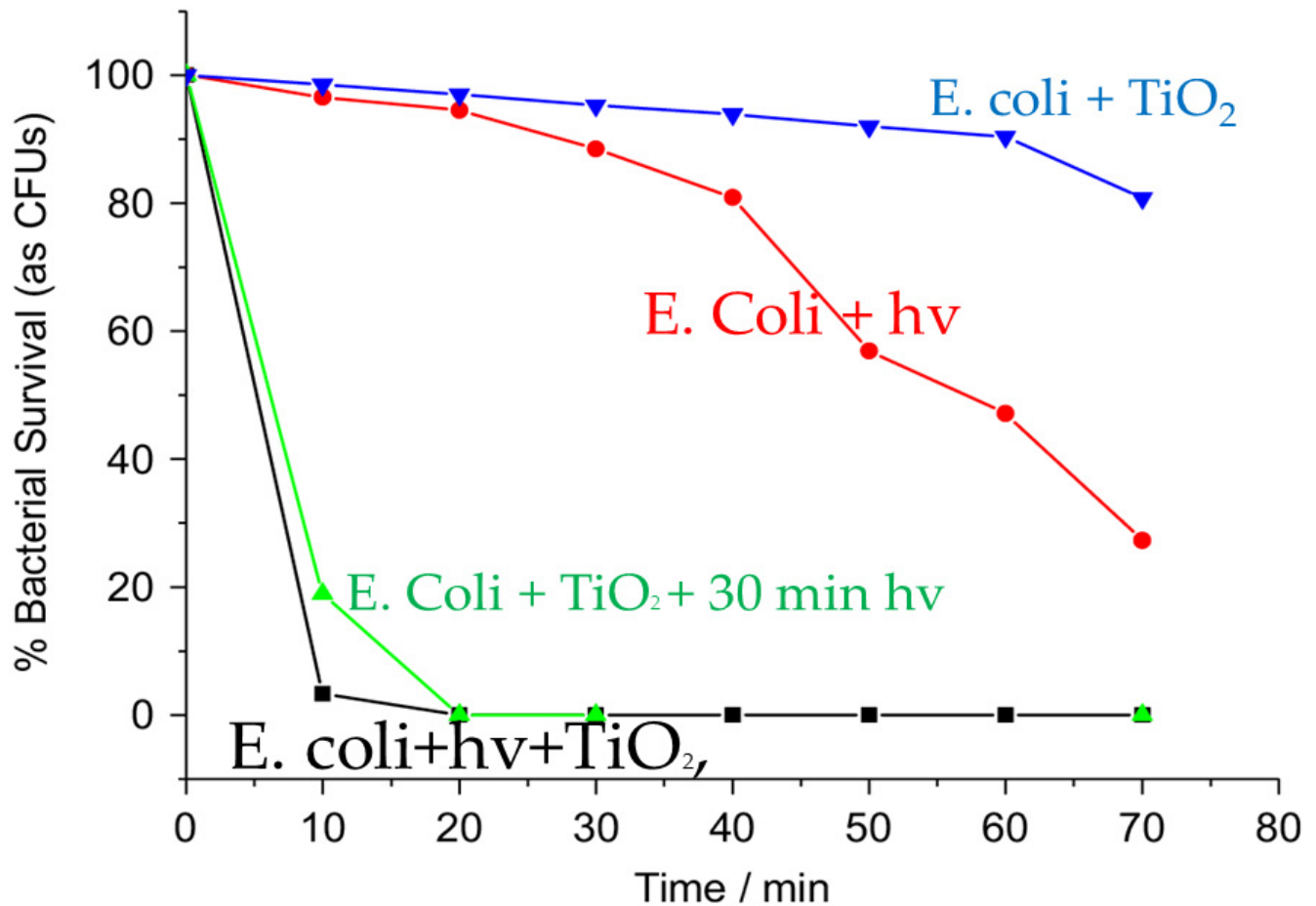


**Figure 8.** *E. coli* cell survival in the presence of  $\text{TiO}_2$  nanocontainers for *E. coli* +  $\text{TiO}_2$ , *E. coli* +  $h\nu$ , *E. coli* +  $\text{TiO}_2$  + 30 min  $h\nu$  and *E. coli* +  $h\nu$  +  $\text{TiO}_2$ .

The same experiments were conducted to investigate the antibacterial activity of hollow nanocontainers of cerium molybdenum (CeMo). Again, the hollow nanocontainers were exposed to *E. coli* culture. The study established parameters such as irradiation and time on the antibacterial activity of hollow nanospheres. Figure 9 shows the results of these studies [46]. One can perceive from this work that the *E. coli* cells in the presence of CeMo nanocontainers diminish after 10 min with or without exposure to the light. The CeMo is a “zero-light” antibacterial compound in the form of a nanocontainer, offering applications in the transport industry, etc.

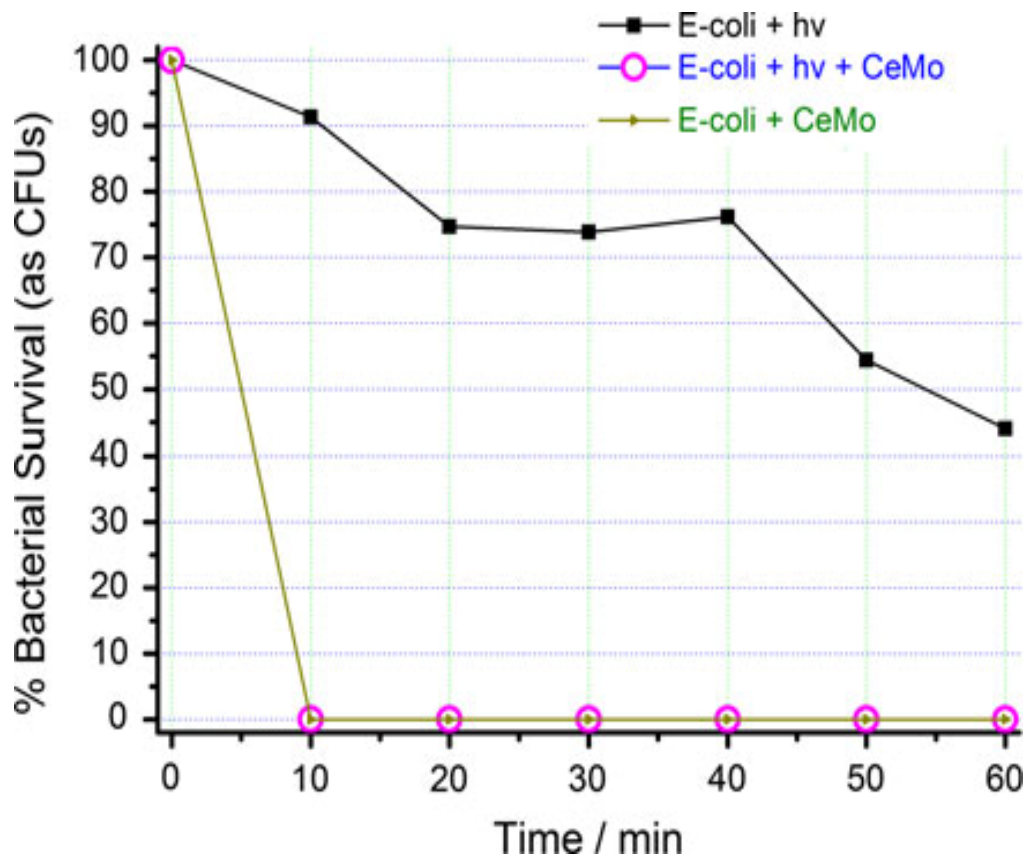


**Figure 9.** Bacterial survival in CeMo hollow nanospheres' presence with or without light illumination.

### 3.4. Energy

Thermal energy storage can be carried out in two ways: with latent heat systems (LHS) or thermal energy storage (TES) systems. For LHS, storage is achieved by heat dissipation or by release through a change in the phase of the material. The high energy density and the narrow range of temperature make these materials effective in various applications. Organic phase-change materials include paraffin waxes, fatty acids, and polyethylene glycol. However, they cannot be used freely on devices because of the leakage they sustain that causes severe damage to the device. One solves this problem when LHS materials such as paraffin are trapped in nano- or microcontainers to store the working substance and do not escape into their incorporated material [56].

#### Nanocontainers Encapsulating PCMs

Implementing the material phase change (PCMs) in thermal energy storage gained significant attention due to the increase in energy consumption and the rescue of the environment from pollution. PCMs absorb, store, and release large amounts of latent heat at specified temperature ranges while phase changes improve device energy efficiency. Depending on the application, the size of the PCMs is selected. Typically, PCMs are classified into nanoPCMs, microPCMs, and macroPCMs, depending on the diameter. The size of the microPCMs usually varies from 1 mm to 1 mm, while capsules less than 100 nm are classified as nanoPCMs and capsules greater than 1 mm as macroPCMs. Encapsulated phase-change materials (EPCM) consist of PCMs with polymer cores and inorganic shells. Microcapsules and nanocapsules containing N-Octadecane in the melamine-formaldehyde shell are manufactured from spot polymerization.

The effects of stirring, the emulsifier's content, the cyclohexane's diameters, morphology, phase-change properties, and thermal stability of PCMs are studied using FT-IR, SEM, DSC, and TGA. For mass production, one can use the spray-drying technique. One can



also use the sol–gel method for their production [3]. In this study, the group observed for the latent heat a value of 156 J/g for paraffin and 80% encapsulation into the SiO<sub>2</sub> containers. In a recent survey, n-octadecane paraffin wax as PCM was studied theoretically and experimentally in nanocontainers in terms of size and conditions of measurements. They observed a thin layer of melted PCM between the hot container wall and solid PCM. The concrete PCM sank and the liquid rose to the sphere's top half. Then, the natural convection became dominant at the top half of the sphere, where the melting rate was lower than the bottom half, causing a reduction in the heat transfer and melting rate in general. Encapsulation sealed the nanoparticles to prevent paraffin from being eliminated, and the process was repeated for many cycles [57]. This improvement in nanofluids' heat transfer coefficient impacts the size of the absorbent surface, water-heating time in a water heater, etc. An innovative method was described to encapsulate high-temperature PCM (salts and eutectics, NaNO<sub>3</sub>, KNO<sub>3</sub>, NaNO<sub>3</sub>-KNO<sub>3</sub>, NaNO<sub>3</sub>-KNO<sub>3</sub>-LiNO<sub>3</sub>) melt in the 120–350 °C temperature range [58]. The study was started to manufacture encapsulated PCMs that can endure the highly corrosive environment of molten alkali metal nitrate-based salts and their eutectics. The established technique does not need a sacrificial layer to lodge the volumetric expansion of the PCMs on melting and reduces the chance of metal corrosion inside the capsule. The encapsulation consists of coating a nonreactive polymer over the PCM pellet, followed by the deposition of a metal layer by a novel nonvacuum (more practical and economically feasible) metal deposition technique (for large-scale fabrication of capsules utilizing commercially available electroless and electroplating chemistry). The fabricated capsules survived more than 2200 thermal cycles (5133 h, equivalent to about 7 years of power plant service) [59]. The thermal cycling test showed no significant degradation in the thermophysical properties of the capsules and PCM on cycling at any testing stage [59].

### 3.5. Biomaterials

Today, there is a significant need for implants due to the large percentage of diseases, the treatment of which is mainly carried out by a surgical procedure. As far as the surgical procedure is concerned, there is excellent evolution due to the advanced antibiotics, new anesthetics, and stable implants for treating bone defects and motor problems. We call biomaterials the implants made by humans. Their use requires biocompatibility with the body, i.e., not causing thrombosis and toxic or allergic inflammations when used as implants in vital tissue. Furthermore, biomaterials must be stable on the surface of contact with the tissues to avoid breakage. Unfortunately, they do not heal themselves like tissues, which determines the time of their life and proper functioning.

Another category of biomaterials, which we call bioactive, react with their surface during contact with their normal body fluids, through which they develop a bond with the bone and tissues, with the result that the organism assimilates them. L. Hench prepared the first bioactive material in 1971 [60–62]. These materials are regenerative because they can suck and regenerate from the bones without leaving residues and are based on silica, calcium, phosphorus, and sodium elements. These materials should be cell-growth drivers facilitated by having a porous size of 100 µm [15,63]. These materials produce links with the tissues and are histogenic. The material produces only extracellular occlusion on its surface, and its surface is flooded by embryonic cells. A great premise is that these materials are prepared easily, repetitively, and economically. In a relatively recent paper, the synthesis of nanocontainers of the SiO<sub>2</sub>-CaO-P<sub>2</sub>O<sub>5</sub> (SiCaP) system was performed with a relatively high concentration in Ca and P. The outer diameter was 330 nm and the thickness of the shell was 40 nm, leaving a cavity of about 250 nm. These properties, with their composition, make them candidates for bone tissue-regeneration applications. In another work, nanocontainers of systems: SiO<sub>2</sub>-CaO, SiO<sub>2</sub>-Na<sub>2</sub>OSiO<sub>2</sub>-P<sub>2</sub>O<sub>5</sub>-CaO, and SiO<sub>2</sub>-P<sub>2</sub>O<sub>5</sub>-Na<sub>2</sub>O were produced, and their osteogenic properties were examined [6]. Treatments in body fluid revealed their osteogenic properties due to the development of a surface-induced hydroxyapatite layer that resembled in structure the naturally occurring apatite component of bone, enhancing

bone development. These systems can be candidates for osteogenic applications tackling bone pathologies such as metabolic bone disease, trauma, and bone cancer ablation.

3.6. Cement

Reinforced concrete is a composite material that results from concrete reinforcement with other materials of greater strength. For example, steel in the form of rods is usually used as a reinforcement, and more rarely, fibers of glass, polymeric materials, and others. The aim is to combine the properties of the above materials into a new one that will meet the needs of the construction. The main disadvantage of concrete is its insufficient tensile strength. Therefore, the reinforcing material must have a high tensile strength to cover the concrete's weakness. In addition, the reinforcing material must have a similar coefficient of thermal expansion. Steel has both of these properties (Figure 10A). On the other hand, a disadvantage of steel is its susceptibility to corrosion (rust) and fire (Figure 10B).

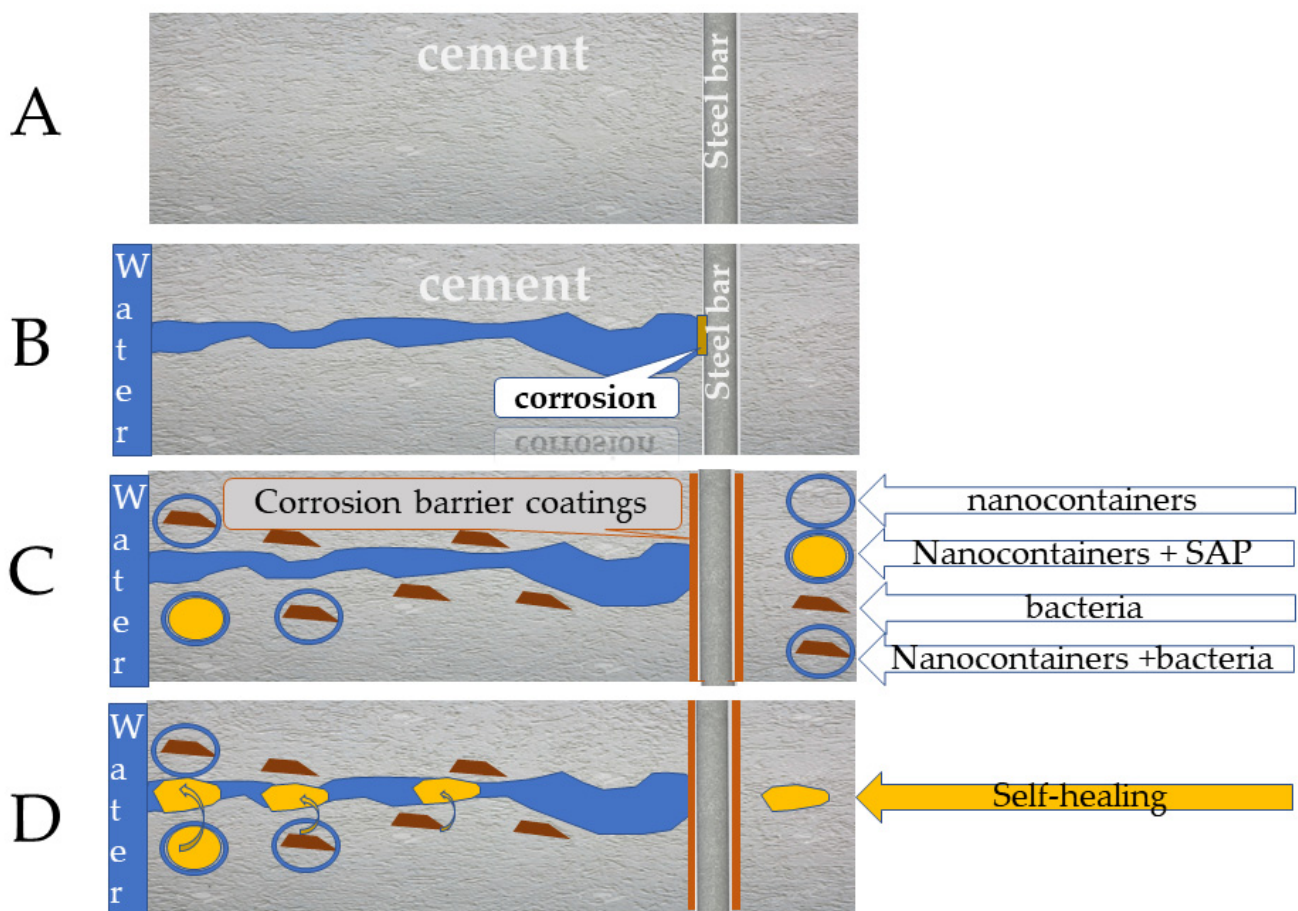


**Figure 10.** Self-healing mechanism in concrete via bacteria and SAP in nanocontainers. (A) Concrete; (B) Concrete with crack, water induces corrosion on steel; (C) Concrete with bacteria, SAP, Nanocontainers filled with SAP or Bacteria; (D) Self-healing.

The microstructure of concrete is porous, which can be isolated or interconnected. Interconnected pores allow water and chemicals to penetrate the concrete. One can understand that permeability plays a vital role in the wear mechanism of concrete. Interconnected pores allow water and chemical compounds to penetrate the concrete matrix. Moreover, CO<sub>2</sub> penetrates the pores to form the cement's alkaline components, e.g., Ca(OH)<sub>2</sub>. This makes it clear that the number of pores must be reduced to limit the movement of harmful substances into the uterus, resulting in iron corrosion. The bibliography has recently developed iron protection technology with ORMOSIL coatings reinforced with CeO<sub>2</sub> (5-ATDT) nanocontainers. These coatings significantly increase metal protection from corrosion and

the appearance of the self-healing effect. Recently, the biological restoration technique has reduced the occlusion of newly formed cracks by introducing bacteria into the concrete. Figure 10C schematically presents this technology. This technology is based on incorporating a bacterium that metabolizes urea and immerses  $\text{CaCO}_3$  in the crack environment. Microbial immersion of  $\text{CaCO}_3$  is certified by several factors, such as the concentration of dissolved inorganic carbonate ions and the concentration of  $\text{Ca}^{2+}$  ions. Bacteria are protected from cement by encapsulation in microcontainers that do not show toxicity.

The spherical poly(methacrylic acids) microspheres of  $\sim 700 \mu\text{m}$  diameter were prepared by distillation–precipitation polymerization. The conversion of carboxylic groups followed this into their sodium salts by treatment with an aqueous sodium hydroxide solution. Figure 11 shows that these water-trap spheres can absorb water 70 times their weight. The absorption and drying cycles are repeated countless times.

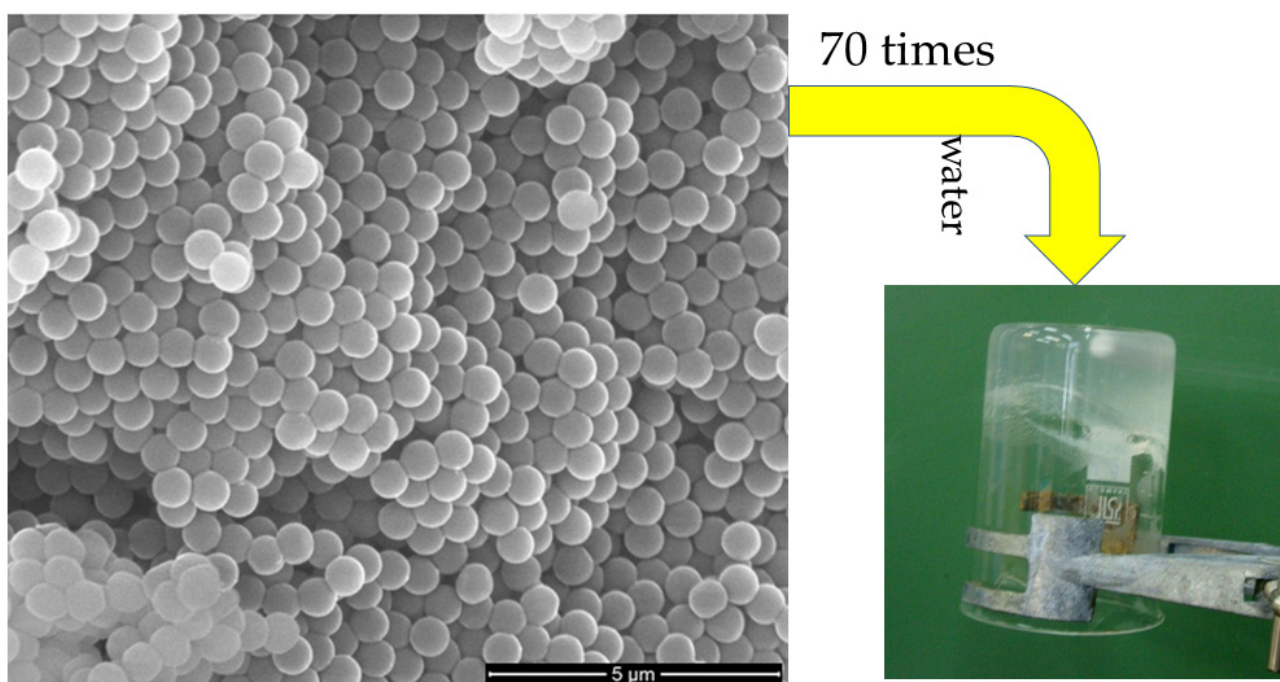


**Figure 11.** SEM images of water traps capable of absorbing water 70 times their weight.

A recent study expanded previous work and produced  $\text{P(MAA-co-EGDMA)@SiO}_2$  by copolymerizing methacrylic acid (MAA) with ethylene glycol dimethacrylate (EGDMA) embedded in the cement slurry, which was found to maintain its structure by exhibiting chemical compatibility with it [16]. The production of  $\text{P(MAANa-co-EGDMA)@CaO-SiO}_2$  was an extension of the initial study. Flexural strength and compressive strength of cement-based composites were measured with concentrations bwoc: 0% SAPs, 0.5% SAPs, and 2% SAPs where it was 1.05 MPa, 1.51 MPa, and 1.83 MPa and 63.68 MPa, 59.67 MPa, and 56.27 MPa, respectively. Cracks of cement composites with 2% SAPs healed after 28 days [64].

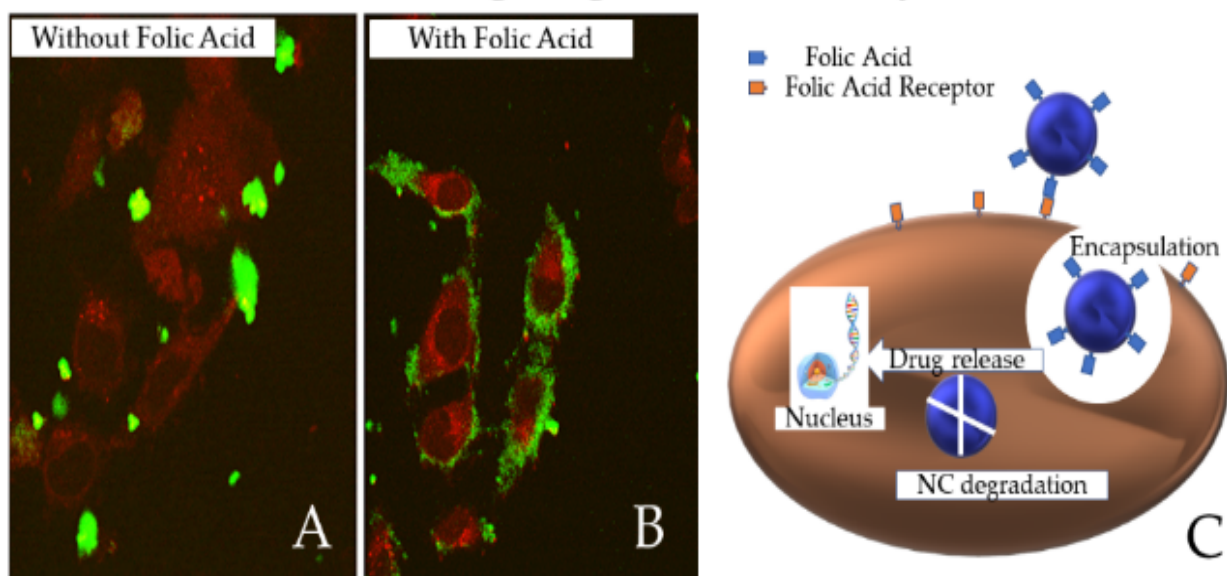
### 3.7. Nanomedicine

When a person is diagnosed with cancer, doctors suggest three treatments: surgery, chemotherapy, and radiotherapy. All solutions are painful, with visible and invisible results. The visual effect of chemotherapy is hair loss, heart dysfunction, and many other unfortunate consequences for the patient. Chemotherapy causes a problem to the organs because a small part of the drugs ends up in cancer sites, and a significant fraction of the organs cause severe damage to their functionality. The question is: how can nanomedicine help alleviate the chemotherapy problem? To begin the discussion, let us answer the question: Is cancer the same as other healthy cells? The answer is: no! Cancer has different

temperature, pH, and redox values than healthy cells [19,20,65–68]. Can nanocontainers recognize that environment and deliver the chemotherapy drug locally? Another question is: Can nanocontainers target only cancer and provide the drug locally? The answer is yes if we use the nanocontainers of Figure 1. The shell of the Nano4XX platform consists of three polymers sensitive to temperature, pH, and redox. This platform contains magnetic nanoparticles for hyperthermia and targeting groups (folic acid for breast cancer, leuprolide for prostate cancer). The targeting groups can attach cancer-terminating groups, and via endocytosis can help the Nano4XX platform to enter cancer cells. The Nano4XX platform exhibits the same T, pH, and redox as cancer, so they can expand inside cancer and deliver the drug locally.

The realization of this technology involved several individual steps [1,7,19,69–72]. Extensive toxicological studies were conducted on animals [73]. We proved the targeting of cancer cells via positron emission tomography (PET) studies [19]. Figure 12 shows Nano4XX (Dox) functionalized with folic acid (F.A.) to target the cancer cells (HeLa) overexpressed at the surface of the explicit hormone. The nanocontainers enter the cancer cells, illuminating the cells red via Dox. On the contrary, the nanocontainers are not targeted with F.A. on the surface, coloring their site green due to Fitch. DNA replication is canceled by intercalation mode. [74,75] The Nano4XX (Dox) platform enters the cancer cells within 15 min of treatment, contrary to the nonfunctionalized Nano4XX (Dox) platform that agglomerates outside cancer cells.

## Cell studies for targeting to HeLa cells by confocal



Red: Lyso-tracker

Green: Fitch-targeted nanocontainers

**Figure 12.** Cell studies for targeting HeLa cells by confocal microscopy [74,76]. (A) Agglomeration because the Nano4XX platform is not FA grafted (green color Nano4XX); (B) FA grafted Nano4XX color the cancer cell surface green, inside the cancer cells are colored red due to Doxorubicin; (C) FA-grafted Nano4Dox enter the cancer cell where they release Doxorubicin inside resulting in a destruction of cancer.

Now that we know that the Nano4XX platform is entering cancer cells, we devised an experiment where the cytotoxicity of the Nano4XX (empty), Nano4Dox platform, and free doxorubicin (0.01, 0.1, 1, 5, 10, and 30  $\mu\text{M}$ ) was studied in the cell lines MCF-7 (breast carcinoma) and HeLa. (Cervical carcinoma) [77]. The F.A. receptor recognizes the HeLa

cells located on their surface. [24–27] Measurements were made after incubating cells in the presence of Nano4XX with or without F.A. for 72 h. Figure 13 shows that Nano4XX (empty) is not toxic to MCF-7 cells for concentrations from 0.01 to 30  $\mu\text{M}$ . However, once Nano4Dox and doxorubicin are encapsulated in cells, cytotoxicity is practiced in both cases. The same results were obtained in HeLa cells, respectively [76].

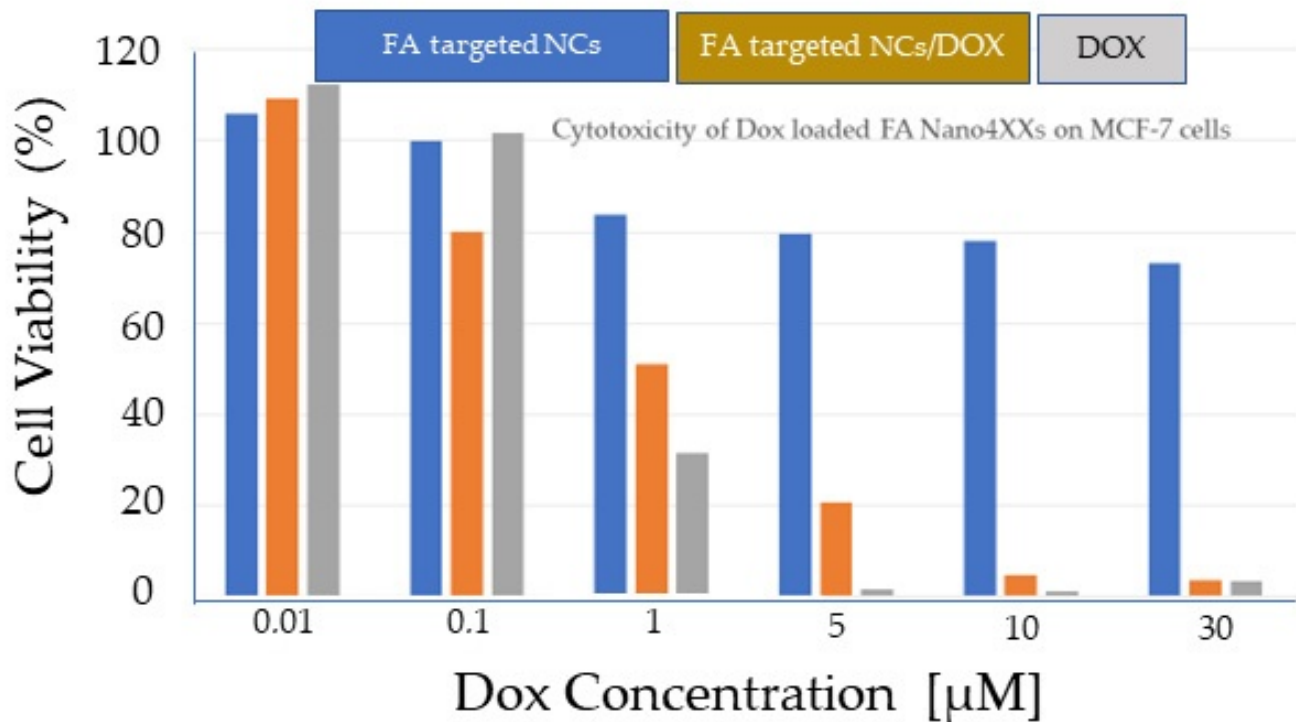


**Figure 13.** Cytotoxicity of F.A.-Nano4XX, FA-Nano4(Dox), and free DOX in MCF-7 cells repeated three times [5,18].

The PET measured Nano4 (Dox) biodistribution with and without F. A. in HeLa mice bearing tumors. Figure 14 shows the distribution of Nano4 (Dox) with or without PET F.A. target groups across various organs and tumors. The measurement was made after a one-hour accumulation where we see the concentration of Nano4 (Dox) in cancer. The concentration in the volume Nano4 (Dox) with F. A. rises to 3.5% after one hour of accumulation [5,18]. Conversely, the attention in the volume without folic acid is zero [21].

Now that we know the Nano4 (Dox) platform with F. A. enters the cancer cells and acts on them; the question is whether they have a therapeutic effect. For this purpose, SCID mice bearing HeLa cervical tumors were studied and used to monitor cancer volume as a function of time in different groups. The experiments were carried out on two types of drugs: doxorubicin and cisplatin. The results are summarized in Figure 15. When the Nano4 (Dox) platform is not equipped with F. A., then there is an increase in cancer volume with time (Figure 15A). The same happens in administering cisplatin to animals with increased volume over time.

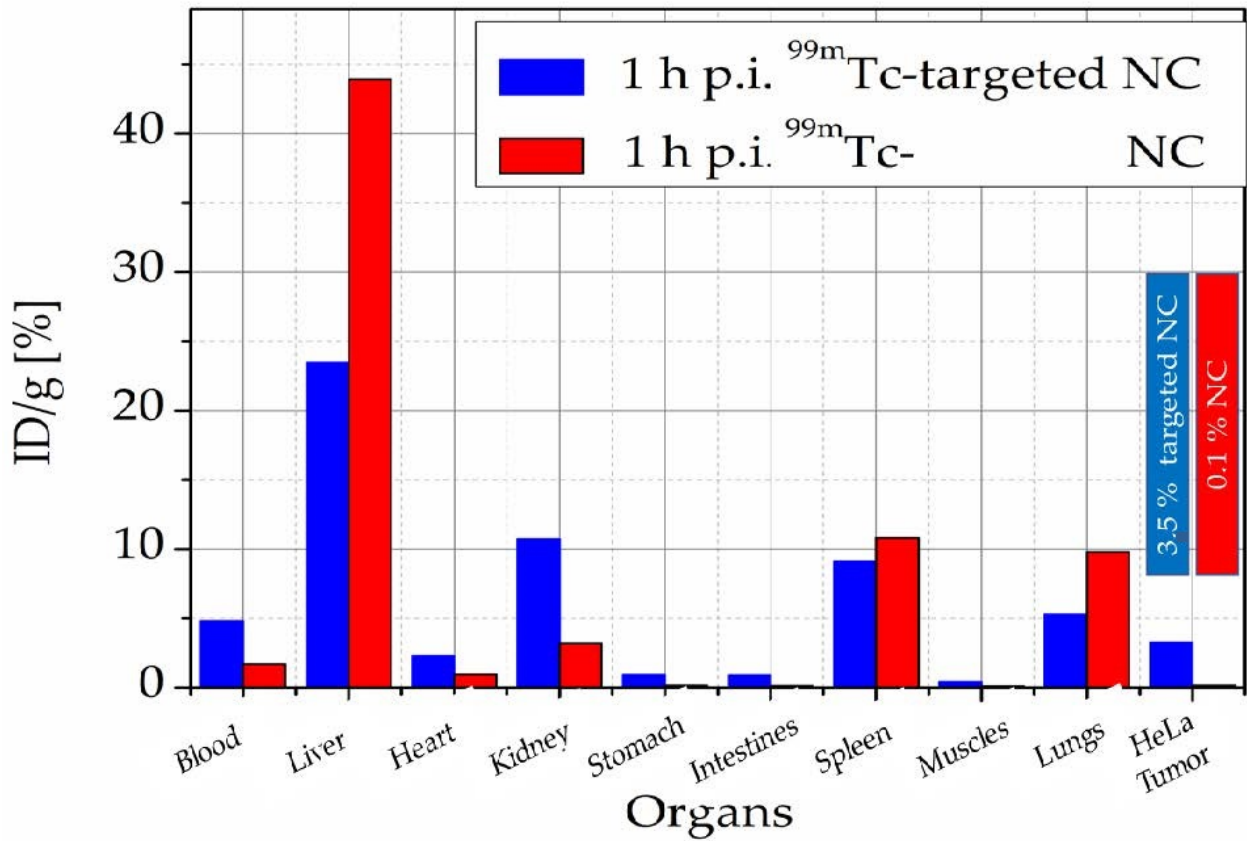


Figure 14. In vivo intake in 1 h in different organs and cancer for Nano4 (Dox) with and without F. A.

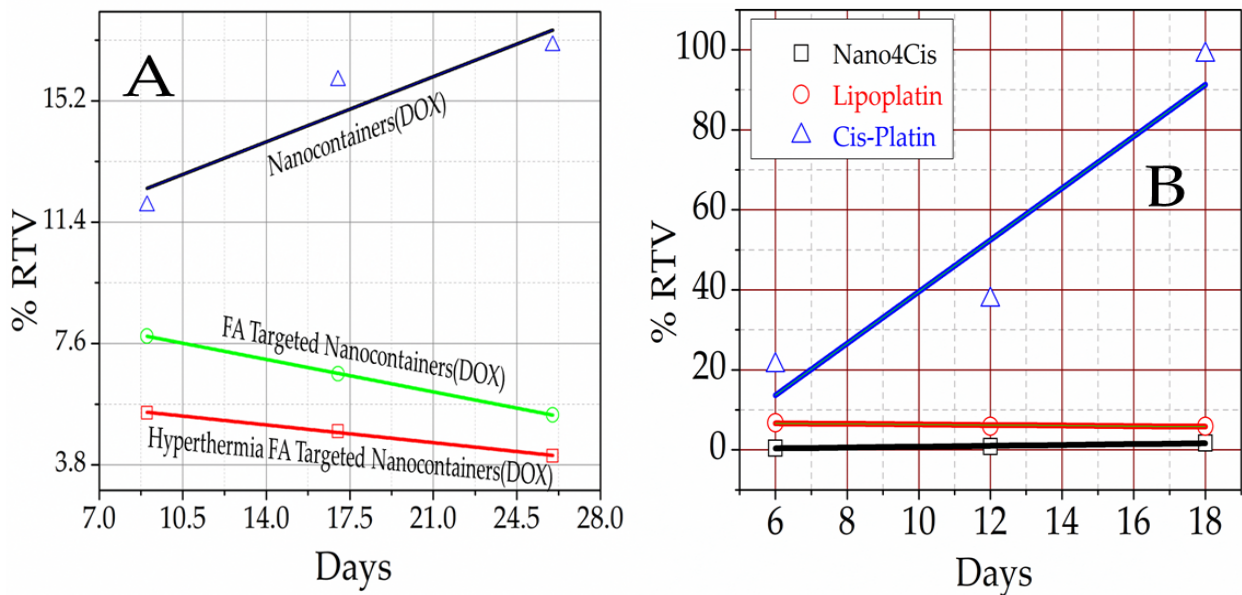


Figure 15. (A) The behavior of Nano4Dox. (Black line) increased cancer volume when nanocontainers were delivered with DOX; (green line) decrease in cancer volume when delivering FA-targeted nanocontainers loaded with DOX; (red line) decrease in cancer volume of FA-targeted nanocontainers loaded with DOX with an application of hyperthermia. (B) (Blue line) Increase in cancer volume when delivering cisplatin; (red line) decrease in cancer volume when producing cisplatin; (black line) further reduction in cancer volume with disposal of Nano4Cis platforms.

In contrast, the volume decreases with time for the Nano4 (Dox) platform when it incorporates the target molecule. In this case, a decrease in cancer volume by 20% is observed in 25 days (Figure 15A). The result is better when hyperthermia is induced in the treatment. The same effect is obtained in the case of the Nano4Cis platform, which shows better results than even lipoplatin. PET measurements have shown that 3.5% attaches to cancer when the Nano4XX platform (Dox, Cis) contains F.A. Toxicological studies and confocal microscopy measurements have found that the Nano4XX platform (Dox, Cis) enters cancer cells and works therapeutically. All these results suggest that the new system is effective in treating cancer. The Nano4XX platform has the intelligence to recognize cancer and act as a system with “artificial intelligence” because it distinguishes healthy cells from cancer cells. These experiments proved that Nano4XX (Dox, Cis) is significantly safer and more effective in vivo than the current gold standard, Doxil© (doxorubicin liposomal), an absolute nanomedical blockbuster in oncology [20,67,78,79]. This Nano4XX (Dox, Cis, etc.) technology has been patented with European and USA patents (see Patents).

#### 4. Conclusions and Perspectives

Every nanocontainer technology has reached a specific technology readiness level (TRL = 1–9). For example, organic nanocontainers present artificial intelligence and have been tested in terms of their therapeutic efficacy with various anticancer drugs, a worldwide patent has been written, and a business plan has been drawn up. However, this technology has a TRL 7 where there must be human studies and GMP production of nanocontainers from now on. Such a Phase I and IIa clinical study costs EUR 10 million and lasts one year. With this, finding a pharmaceutical company to continue the development in the following phases will be straightforward.

The antifouling paint technology also has a significant technology readiness level, TRL 7, because the technology was tested on two commercial ships, produced on an industrial scale of the nanocontainers, and supported by a patent, and used ecological antifoulants. After a year of sailing, the vessel partially painted with nanotechnology showed much better results than commercial paints.

The technology of anticorrosion painting metals with CeMo (MBT, 8HQ) nanocontainers was made with the funding of two European projects, MULTIPROTECT and MUST, involving DAIMLER, FIAT, EADS, Chemetal, Mankiewicz, and Sika. Prototypes were made in representative metal parts, where nanotechnology paint technology was demonstrated using parts of automobiles and airplanes with a small mix of nanocontainers. In terms of TRL, this paint technology is very advanced because large companies were involved. It is up to the manufacturers to adopt and promote these technologies.

Other technologies, such as nanocontainers in biomaterials, cement self-healing, energy storage, and antimicrobial technology, are in the run-up but are promising technologies. In addition, discussions with industrial partners and funding agencies are underway to develop these technologies further. However, many questions have not been answered regarding the lifetime of these technologies. For example, a building requires the incorporation of self-healing nanocontainers at a time that has not been convincingly verified until today. Furthermore, as far as SiO<sub>2</sub> (paraffin) PCMs are concerned, there are problems with exploiting paraffin by leakage of the nanocontainers that limit their lifetime to applications.

All these achievements, with a research effort of many researchers who have understood the opportunities offered by the nanocontainers, will soon be flooding the commercial world with nanocontainer-based products benefiting human beings. I hope this review will incentivize researchers to engage in this field with many innovations.

#### 5. Patents

W.O. 2015/074762 A1, US2016263221, “MULTI-RESPONSIVE TARGETING DRUG DELIVERY SYSTEMS FOR CONTROLLED-RELEASE PHARMACEUTICAL FORMULATION”.

**Funding:** Support by the grant Self-Healing Construction Materials (contract No. 075-15-2021-590 dated 4 June 2021) is greatly appreciated. The Nano4XX platforms were developed under the two IDEAS ERC Grants with the project acronyms Nanotherapy and grant numbers 232959 (AdG) and 620238 (PoC).

**Institutional Review Board Statement:** Not applicable.

**Informed Consent Statement:** Not applicable.

**Data Availability Statement:** Not applicable.

**Acknowledgments:** The author is thankful for support from the grant Self-Healing Construction Materials (Contract Nos. 075-15-2021-590 dated 4 June 2021).

**Conflicts of Interest:** There are no conflict of interest.

## References

1. Tapeinos, C.; Efthimiadou, E.K.; Boukos, N.; Kordas, G. Sustained release profile of quatro stimuli nanocontainers as a multi sensitive vehicle exploiting cancer characteristics. *Colloids Surf. B Biointerfaces* **2016**, *148*, 95–103. [[CrossRef](#)] [[PubMed](#)]
2. Kordas, G. Corrosion Barrier Coatings: Progress and Perspectives of the Chemical Route. *Corros. Mater. Degrad.* **2022**, *3*, 376–413. [[CrossRef](#)]
3. Belessiotis, G.V.; Papadokostaki, K.G.; Favvas, E.P.; Efthimiadou, E.K.; Karellas, S. Preparation and investigation of distinct and shape stable paraffin/SiO<sub>2</sub> composite PCM nanospheres. *Energy Convers. Manag.* **2018**, *168*, 382–394. [[CrossRef](#)]
4. Kordas, G. Nanocontainers Against Biofouling and Corrosion Degradation of Materials: A Short Review With Prospects. *Front. Nanotechnol.* **2022**, *4*, 1–13. [[CrossRef](#)]
5. Kordas, G.; Efthimiadou, E.K. Self-Healing Coatings for Corrosion Protection of Metals. *Sol-Gel Handb.* **2015**, *3*, 1371–1384. [[CrossRef](#)]
6. Angelopoulou, A.; Efthimiadou, E.K.; Kordas, G. A new approach to fabricate bioactive silica binary and ternary hybrid microspheres. *Mater. Sci. Eng. C* **2015**, *53*, 76–82. [[CrossRef](#)]
7. Tapeinos, C.; Kartsonakis, I.; Liatsi, P.; Daniilidis, I.; Kordas, G. Synthesis and characterization of magnetic nanocontainers. *J. Am. Ceram. Soc.* **2008**, *91*, 1052–1056. [[CrossRef](#)]
8. Kordas, G. Protection of HDG Steel Using ORMOSIL Coatings Enhanced with CeO (5-ATDT)-Ceramic Nanocontainers. *Appl. Sci. Eng. Prog.* **2022**, *16*, 6329. [[CrossRef](#)]
9. Li, D.; Wang, F.; Yu, X.; Wang, J.; Liu, Q.; Yang, P.; He, Y.; Wang, Y.; Zhang, M. Anticorrosion organic coating with layered double hydroxide loaded with corrosion inhibitor of tungstate. *Prog. Org. Coat.* **2011**, *71*, 302–309. [[CrossRef](#)]
10. Shchukina, E.; Shchukin, D.G. Nanocontainer-Based Active Systems: From Self-Healing Coatings to Thermal Energy Storage. *Langmuir* **2019**, *35*, 8603–8611. [[CrossRef](#)]
11. Mekeridis, E.D.; Kartsonakis, I.A.; Pappas, G.S.; Kordas, G.C. Release studies of corrosion inhibitors from cerium titanium oxide nanocontainers. *J. Nanoparticle Res.* **2011**, *13*, 541–554. [[CrossRef](#)]
12. Kordas, G. ORMOSIL Coatings Enriched with CeO<sub>2</sub> (5-ATDT)-Ceramic Nanocontainers for Enhanced Protection of HDG Steel Used in Concrete. *Materials* **2022**, *15*, 3913. [[CrossRef](#)] [[PubMed](#)]
13. Mekeridis, E.D.; Kartsonakis, I.A.; Kordas, G.C. Multilayer organic-inorganic coating incorporating TiO<sub>2</sub> nanocontainers loaded with inhibitors for corrosion protection of AA2024-T3. *Prog. Org. Coat.* **2012**, *73*, 142–148. [[CrossRef](#)]
14. Kordas, G.C.; Balaskas, A.C.; Kartsonakis, I.A.; Efthimiadou, E.K. A Raman study of 8-Hydroxyquinoline release from loaded TiO<sub>2</sub> nanocontainer. *Int. J. Struct. Integr.* **2013**, *4*, 121–126. [[CrossRef](#)]
15. Pappas, G.S.; Liatsi, P.; Kartsonakis, I.A.; Daniilidis, I.; Kordas, G. Synthesis and characterization of new SiO<sub>2</sub>-CaO hollow nanospheres by sol-gel method: Bioactivity of the new system. *J. Non-Cryst. Solids* **2008**, *354*, 755–760. [[CrossRef](#)]
16. Kanellopoulou, I.; Karaxi, E.K.; Karatza, A.; Kartsonakis, I.A.; Charitidis, C. Hybrid superabsorbent polymer networks (SAPs) encapsulated with SiO<sub>2</sub> for structural applications. *MATEC Web Conf.* **2018**, *188*, 01025. [[CrossRef](#)]
17. Karatzas, A.; Bilalis, P.; Kartsonakis, I.A.; Kordas, G.C. Reversible spherical organic water microtraps. *J. Non-Cryst. Solids* **2012**, *358*, 443–445. [[CrossRef](#)]
18. Krzak, M.; Tabor, Z.; Nowak, P.; Warszyński, P.; Karatzas, A.; Kartsonakis, I.A.; Kordas, G.C.; Warszy, P.; Karatzas, A.; Kartsonakis, I.A.; et al. Water diffusion in polymer coatings containing water-trapping particles. Part 2. Experimental verification of the mathematical model. *Prog. Org. Coat.* **2012**, *75*, 207–214. [[CrossRef](#)]
19. Kordas, G. Quadrupole Stimuli-Responsive Targeted Polymeric Nanocontainers for Cancer Therapy: Artificial Intelligence in Drug Delivery Systems. *Nanoeng. Biomater.* **2022**, *1*, 505–522. [[CrossRef](#)]
20. Kordas, G. *Nanotechnology in Cancer Treatment as a Trojan Horse: From the Bench to Preclinical Studies*; Sarat Kumar Swain, M.J., Ed.; Elsevier Inc.: London, UK, 2019; ISBN 9780128167717.
21. Rollett, A.; Reiter, T.; Nogueira, P.; Cardinale, M.; Loureiro, A.; Gomes, A.; Cavaco-Paulo, A.; Moreira, A.; Carmo, A.M.; Guebitz, G.M. Folic acid-functionalized human serum albumin nanocapsules for targeted drug delivery to chronically activated macrophages. *Int. J. Pharm.* **2012**, *427*, 460–466. [[CrossRef](#)]



22. Montemor, M.F.; Snihirova, D.V.; Taryba, M.G.; Lamaka, S.V.; Kartsonakis, I.A.; Balaskas, A.C.; Kordas, G.C.; Tedim, J.; Kuznetsova, A.; Zheludkevich, M.L.; et al. Evaluation of self-healing ability in protective coatings modified with combinations of layered double hydroxides and cerium molybdate nanocontainers filled with corrosion inhibitors. *Electrochim. Acta* **2012**, *60*, 31–40. [[CrossRef](#)]
23. Poornima Vijayan, P.; Al-Maadeed, M.A.S.A. TiO<sub>2</sub> nanotubes and mesoporous silica as containers in self-healing epoxy coatings. *Sci. Rep.* **2016**, *6*, 38812. [[CrossRef](#)] [[PubMed](#)]
24. Kordas, G. Nanocontainers-Based Anti-Biofouling Coatings—A Pilot Study. *Supramol. Chem. Corros. Biofouling Prot.* **2021**, 383–392. [[CrossRef](#)]
25. Kordas, G. Nanocontainers (CeO<sub>2</sub>): Synthesis, Characterization, Properties, and Anti-corrosive Application. In *Sustainable Corrosion Inhibitors II: Synthesis, Design, and Practical Applications*; ACS Symposium Series; Hussain, C.M., Verma, C., Aslam, J., Eds.; American Chemical Society: Washington, DC, USA, 2021; Chapter 8; pp. 177–185. [[CrossRef](#)]
26. Kordas, G. Nanotechnology to improve the biofouling and corrosion performance of marine paints: From lab experiments to real tests in sea. *Int. J. Phys. Res. Appl.* **2019**, *2*, 033–037. [[CrossRef](#)]
27. Kartsonakis, I.; Daniilidis, I.; Kordas, G. Encapsulation of the corrosion inhibitor 8-hydroxyquinoline into ceria nanocontainers. *J. Sol-Gel Sci. Technol.* **2008**, *48*, 24–31. [[CrossRef](#)]
28. Kartsonakis, I.A.; Athanasopoulou, E.; Snihirova, D.; Martins, B.; Koklioti, M.A.; Montemor, M.F.; Kordas, G.; Charitidis, C.A. Multifunctional epoxy coatings combining a mixture of traps and inhibitor loaded nanocontainers for corrosion protection of AA2024-T3. *Corros. Sci.* **2014**, *85*, 147–159. [[CrossRef](#)]
29. Kordas, G. CuO (Bromosphaerol) and CeMo (8 Hydroxyquinoline) microcontainers incorporated into commercial marine paints. *J. Am. Ceram. Soc.* **2020**, *103*, 2340–2350. [[CrossRef](#)]
30. Aldred, N.; Clare, A.S. The adhesive strategies of cyprids and development of barnacle-resistant marine coatings. *Biofouling* **2008**, *24*, 351–363. [[CrossRef](#)]
31. Guezennec, J.; Herry, J.M.; Kouzayha, A.; Bachere, E.; Mittelman, M.W.; Bellon Fontaine, M.N. Exopolysaccharides from unusual marine environments inhibit early stages of biofouling. *Int. Biodeterior. Biodegrad.* **2012**, *66*, 1–7. [[CrossRef](#)]
32. Qian, P.; Lau, S.C.K.; Dahms, H.; Dobretsov, S.; Harder, T. Invited Review Marine Biofilms as Mediators of Colonization by Marine Macroorganisms: Implications for Antifouling and Aquaculture. *Mar. Biotechnol.* **2007**, *9*, 399–410. [[CrossRef](#)]
33. Magin, C.M.; Cooper, S.P.; Brennan, A.B. The term fouling generally refers to an undesirable process in which relate to the initial attachment of fouling organisms. *Mater. Today* **2010**, *13*, 36–44. [[CrossRef](#)]
34. Bidwell, J.R.; Cherry, D.S.; Farris, J.L.; Petrille, J.C.; Lyons, L.A. Effects of intermittent halogenation on settlement, survival and growth of the zebra mussel, *Dreissena polymorpha*. *Hydrobiologia* **1999**, *394*, 53–62. [[CrossRef](#)]
35. Burgess, J.G.; Boyd, K.G.; Armstrong, E.; Jiang, Z.; Yan, L.; Berggren, M.; May, U.; Pisacane, T.; Granmo, Å.; Adams, D.R. The Development of a Marine Natural Product-based Antifouling Paint. *Biofouling* **2003**, *19*, 197–205. [[CrossRef](#)] [[PubMed](#)]
36. Rittschof, D.A.N. Natural product antifoulants: One perspective on the challenges related to coatings development Natural Product Antifoulants: One Perspective on the Challenges Related to Coatings Development. *Biofouling* **2009**, *15*, 37–41.
37. Hay, M.E. Marine chemical ecology: What 's known and what 's next? *J. Exp. Mar. Biol. Ecol.* **2009**, *15*, 119–127. [[CrossRef](#)]
38. Chapman, J.; Hellio, C.; Sullivan, T.; Brown, R.; Russell, S.; Kitteringham, E.; Le Nor, L.; Regan, F. Bioinspired synthetic macroalgae: Examples from nature for antifouling applications. *Int. Biodeterior. Biodegrad.* **2014**, *86*, 6–13. [[CrossRef](#)]
39. Pawlik, J.R. The Development of a Marine Natural Product-based Antifouling Paint. *Oceanogr. Mar. Biol. Rev.* **1992**, *30*, 273–335.
40. Grandgirard, J.; Poinot, D.; Krespi, L.; Nénon, J.P.; Cortesero, A.M. Chemical ecology of marine microbial defence. *J. Chem. Ecol.* **2002**, *103*, 1971–1985. [[CrossRef](#)]
41. Hellio, C.; Berge, J.P.; Beaupoil, C.; Le Gal, Y.; Bourgougnon, N. Screening of marine algal extracts for anti-settlement activities against microalgae and macroalgae. *Biofouling* **2002**, *18*, 205–215. [[CrossRef](#)]
42. Kordas, G. Novel Antifouling and Self-Healing Eco-Friendly Coatings for Marine Applications Enhancing the Performance of Commercial Marine Paints. In *Engineering Failure Analysis*; Thanapalan, K., Ed.; IntechOpen: London, UK, 2020; pp. 1–9.
43. Krishna Mohan, M.V.; Bhanuprakash, T.V.K.; Mukherjee, A. Al<sub>2</sub>O<sub>3</sub> and CuO nano particulate-based paints for marine applications. *Eng. Res. Express* **2022**, *4*, 035056. [[CrossRef](#)]
44. Qing, Y.; Long, C.; An, K.; Liu, C. Natural rosin-grafted nanoparticles for extremely-robust and eco-friendly antifouling coating with controllable liquid transport. *Compos. Part B Eng.* **2022**, *236*, 109797. [[CrossRef](#)]
45. Chen, X.; Cui, Z.; Chen, Z.; Zhang, K.; Lu, G.; Zhang, G.; Yang, B. The synthesis and characterizations of monodisperse cross-linked polymer microspheres with carboxyl on the surface. *Polymer* **2002**, *43*, 4147–4152. [[CrossRef](#)]
46. Kartsonakis, I.A.; Kontogiani, P.; Pappas, G.S.; Kordas, G. Photocatalytic action of cerium molybdate and iron-titanium oxide hollow nanospheres on *Escherichia coli*. *J. Nanoparticle Res.* **2013**, *15*, 1–10. [[CrossRef](#)]
47. Kartsonakis, I.A.; Liatsi, P.; Danilidis, I.; Bouzarelou, D.; Kordas, G. Synthesis, characterization and antibacterial action of hollow titania spheres. *J. Phys. Chem. Solids* **2008**, *69*, 214–221. [[CrossRef](#)]
48. Eiden, S.; Maret, G. Preparation and characterization of hollow spheres of rutile. *J. Colloid Interface Sci.* **2002**, *250*, 281–284. [[CrossRef](#)]
49. Wang, D.; Song, C.; Lin, Y.; Hu, Z. Preparation and characterization of TiO<sub>2</sub> hollow spheres. *Mater. Lett.* **2006**, *60*, 77–80. [[CrossRef](#)]
50. Song, C.; Wang, D.; Gu, G.; Lin, Y.; Yang, J.; Chen, L.; Fu, X.; Hu, Z. Preparation and characterization of silver/TiO<sub>2</sub> composite hollow spheres. *J. Colloid Interface Sci.* **2004**, *272*, 340–344. [[CrossRef](#)]

51. Shiho, H.; Kawahashi, N. Iron compounds as coatings on polystyrene latex and as hollow spheres. *J. Colloid Interface Sci.* **2000**, *226*, 91–97. [[CrossRef](#)]
52. Zhao, Y.; Liu, J.; Liu, Q.; Sun, Y.; Song, D.; Yang, W.; Wang, J.; Liu, L. One-step synthesis of SnO<sub>2</sub> hollow microspheres and its gas sensing properties. *Mater. Lett.* **2014**, *136*, 286–288. [[CrossRef](#)]
53. Cai, J.; Wu, X.; Zheng, F.; Li, S.; Wu, Y.; Lin, Y.; Lin, L.; Liu, B.; Chen, Q.; Lin, L. Influence of TiO<sub>2</sub> hollow sphere size on its photo-reduction activity for toxic Cr(VI) removal. *J. Colloid Interface Sci.* **2017**, *490*, 37–45. [[CrossRef](#)]
54. Jackson, G.J.; Merker, R.I.; Bandler, R. *Bacteriological Analytical Manual*; U.S. Food & Drug Administration Center for Food Safety & Applied Nutrition Bacteriological: Silver Spring, MD, USA, 2001.
55. Kartsonakis, I.A.; Liatsi, P.; Daniilidis, I.; Kordas, G. Synthesis, characterization, and antibacterial action of hollow ceria nanospheres with/without a conductive polymer coating. *J. Am. Ceram. Soc.* **2008**, *91*, 372–378. [[CrossRef](#)]
56. Umair, M.M.; Zhang, Y.; Iqbal, K.; Zhang, S.; Tang, B. Novel strategies and supporting materials applied to shape-stabilize organic phase change materials for thermal energy storage—A review. *Appl. Energy* **2019**, *235*, 846–873. [[CrossRef](#)]
57. Li, R.; Zhou, Y.; Duan, X. Nanoparticle enhanced paraffin and tailing ceramic composite phase change material for thermal energy storage. *Sustain. Energy Fuels* **2020**, *4*, 4547–4557. [[CrossRef](#)]
58. Roget, F.; Favotto, C.; Rogez, J. Study of the KNO<sub>3</sub>-LiNO<sub>3</sub> and KNO<sub>3</sub>-NaNO<sub>3</sub>-LiNO<sub>3</sub> eutectics as phase change materials for thermal storage in a low-temperature solar power plant. *Sol. Energy* **2013**, *95*, 155–169. [[CrossRef](#)]
59. Wickramaratne, C.; Dhau, J.S.; Kamal, R.; Myers, P.; Goswami, D.Y.; Stefanakos, E. Macro-encapsulation and characterization of chloride based inorganic Phase change materials for high temperature thermal energy storage systems. *Appl. Energy* **2018**, *221*, 587–596. [[CrossRef](#)]
60. Hench, L.L.; Best, S.M. *Chapter I. 2.4 Ceramics, Glasses, and Glass-Ceramics: Basic Principles Types of Bioceramics: Tissue*, 3rd ed.; Elsevier: Amsterdam, The Netherlands, 2004.
61. Hench, L.L. Sol-gel materials for bioceramic. *Curr. Opin. Solid State Mater. Sci.* **1997**, *2*, 604–610. [[CrossRef](#)]
62. Hench, L.L. The story of Bioglass®. *J. Mater. Sci. Mater. Med.* **2006**, *17*, 967–978. [[CrossRef](#)] [[PubMed](#)]
63. Pappas, G.S.; Bilalis, P.; Kordas, G.C. Synthesis and characterization of SiO<sub>2</sub>-CaO-P<sub>2</sub>O<sub>5</sub> hollow nanospheres for biomedical applications. *Mater. Lett.* **2012**, *67*, 273–276. [[CrossRef](#)]
64. Kanellopoulou, I.; Karaxi, E.K.; Karatza, A.; Kartsonakis, I.A.; Charitidis, C.A. Effect of submicron admixtures on mechanical and self-healing properties of cement-based composites. *Fatigue Fract. Eng. Mater. Struct.* **2019**, *42*, 1494–1509. [[CrossRef](#)]
65. Cheng, R.; Meng, F.; Deng, C.; Klok, H.A.; Zhong, Z. Dual and multi-stimuli responsive polymeric nanoparticles for programmed site-specific drug delivery. *Biomaterials* **2013**, *34*, 3647–3657. [[CrossRef](#)]
66. Bilalis, P.; Chatzipavlidis, A.; Tziveleka, L.A.; Boukos, N.; Kordas, G. Nanodesigned magnetic polymer containers for dual stimuli actuated drug controlled release and magnetic hyperthermia mediation. *J. Mater. Chem.* **2012**, *22*, 13451–13454. [[CrossRef](#)]
67. Kordas, G.; Efthimiadou, E. Comparison of therapeutic efficacy of quadrupole stimuli-targeted nanocontainers loaded with Doxorubicin (Nano4Dox platform) and cisplatin (Nano4Cis platform) to Doxil and Lipoplatin, respectively. *Ann. Clin. Pharmacol. Toxicol.* **2018**, *1*, 1–5.
68. Sahoo, B.; Devi, K.S.P.; Banerjee, R.; Maiti, T.K.; Pramanik, P.; Dhara, D. Thermal and pH responsive polymer-tethered multifunctional magnetic nanoparticles for targeted delivery of anticancer drug. *ACS Appl. Mater. Interfaces* **2013**, *5*, 3884–3893. [[CrossRef](#)] [[PubMed](#)]
69. Efthimiadou, E.K.; Fragogeorgi, E.; Palamaris, L.; Karampelas, T.; Lelovas, P.; Loudos, G.; Tamvakopoulos, C.; Kostomitsopoulos, N.; Kordas, G. Versatile quarto stimuli nanostructure based on Trojan Horse approach for cancer therapy: Synthesis, characterization, in vitro and in vivo studies. *Mater. Sci. Eng. C* **2017**, *79*, 605–612. [[CrossRef](#)]
70. Kartsonakis, I.A.; Charitidis, C.A.; Kordas, G.C. Synthesis and characterization of ceramic hollow nanocomposites and nanotraps. *Nanocomposites Mater. Manuf. Eng.* **2013**, *2*, 1–31. [[CrossRef](#)]
71. Efthimiadou, E.K.; Tapeinos, C.; Tziveleka, L.A.; Boukos, N.; Kordas, G. PH- and thermo-responsive microcontainers as potential drug delivery systems: Morphological characteristic, release and cytotoxicity studies. *Mater. Sci. Eng. C* **2014**, *37*, 271–277. [[CrossRef](#)]
72. Efthimiadou, E.K.; Tapeinos, C.; Chatzipavlidis, A.; Boukos, N.; Fragogeorgi, E.; Palamaris, L.; Loudos, G.; Kordas, G. Dynamic in vivo imaging of dual-triggered microspheres for sustained release applications: Synthesis, characterization and cytotoxicity study. *Int. J. Pharm.* **2014**, *461*, 54–63. [[CrossRef](#)]
73. Lelovas, P.; Efthimiadou, E.K.; Mantziaras, G.; Siskos, N.; Kordas, G.; Kostomitsopoulos, N. In vivo toxicity study of quatro stimuli nanocontainers in pregnant rats: Gestation, parturition and offspring evaluation. *Regul. Toxicol. Pharmacol.* **2018**, *98*, 161–167. [[CrossRef](#)]
74. Yang, H.; Lou, C.; Xu, M.; Wu, C.; Miyoshi, H.; Liu, Y. Investigation of folate-conjugated fluorescent silica nanoparticles for targeting delivery to folate receptor-positive tumors and their internalization mechanism. *Int. J. Nanomed.* **2011**, *6*, 2023–2032. [[CrossRef](#)]
75. Roger, E.; Kalscheuer, S.; Kirtane, A.; Guru, B.R.; Grill, A.E.; Whittum-Hudson, J.; Panyam, J. Folic acid functionalized nanoparticles for enhanced oral drug delivery. *Mol. Pharm.* **2012**, *9*, 2103–2110. [[CrossRef](#)]

76. Efthimiadou, E.K.; Lelovas, P.; Fragogeorgi, E.; Boukos, N.; Balafas, V.; Loudos, G.; Kostomitsopoulos, N.; Theodosiou, M.; Tziveleka, A.L.; Kordas, G. Folic acid mediated endocytosis enhanced by modified multi stimuli nanocontainers for cancer targeting and treatment: Synthesis, characterization, in-vitro and in-vivo evaluation of therapeutic efficacy. *J. Drug Deliv. Sci. Technol.* **2020**, *55*, 101481. [[CrossRef](#)]
77. Mosmann, T. Rapid Colorimetric Assay for Cellular Growth and Survival: Application to Proliferation and Cytotoxicity Assays. *J. Immunological Methods* **1983**, *65*, 55–63. [[CrossRef](#)] [[PubMed](#)]
78. Efthimiadou, E.; Tziveleka, L.-A.; Bilalis, P.; Kordas, G. Novel PLA modification of organic microcontainers based on ring opening polymerization: Synthesis, characterization, biocompatibility and drug loading/release properties. *Int. J. Pharm.* **2012**, *428*, 134–142. [[CrossRef](#)] [[PubMed](#)]
79. Kordas, G. Adjustable Quatro Stimuli (T, pH, Redox, Hyperthermia) Targeted Nanocontainers (Nano4Dox and Nano4Cis) for Cancer Therapy Based on Trojan Horse Approach. *Arch. Pharm. Pharmacol. Res.* **2018**, *1*, 1–7. [[CrossRef](#)]